Weak Localization in Mesoscopic Hole Transport: Berry Phases and Classical Correlations

Viktor Krueckl,[1] Michael Wimmer,[2] İnanç Adagideli,[3] Jack Kuipers,[1] and Klaus Richter[1]

[1]*Institut für Theoretische Physik, Universität Regensburg, D-93040 Regensburg, Germany*
[2]*Instituut-Lorentz, Universiteit Leiden, P.O. Box 9506, 2300 RA Leiden, The Netherlands*
[3]*Faculty of Engineering and Natural Sciences, Sabanci University, Istanbul 34956, Turkey*

(Received 28 September 2010; published 4 April 2011)

We consider phase-coherent transport through ballistic and diffusive two-dimensional hole systems based on the Kohn-Luttinger Hamiltonian. We show that intrinsic heavy-hole–light-hole coupling gives rise to clear-cut signatures of an associated Berry phase in the weak localization which renders the magnetoconductance profile distinctly different from electron transport. Nonuniversal classical correlations determine the strength of these Berry phase effects and the effective symmetry class, leading even to antilocalization-type features for circular quantum dots and Aharonov-Bohm rings in the absence of additional spin-orbit interaction. Our semiclassical predictions are confirmed by numerical calculations.

DOI: 10.1103/PhysRevLett.106.146801 PACS numbers: 73.23.−b, 03.65.Sq, 05.45.Mt, 72.15.Rn

As a genuine wave phenomenon, coherent backscattering, denoting enhanced backreflection of waves in complex media due to constructive interference of time-reversed paths, has been encountered in numerous systems. Its occurrence ranges from the observation of the infrared intensity reflected from Saturn's rings [1] to light scattering in random media [2], from enhanced backscattering of seismic [3] and acoustic [4] to atomic matter waves [5]. In condensed matter, weak localization (WL) [6,7], closely related to coherent backscattering, has been widely used as a diagnostic tool for probing phase coherence in conductors at low temperatures. Based on time-reversal symmetry (TRS), WL manifests itself as a characteristic dip in the average magnetoconductivity at zero magnetic field B. The opposite phenomenon, a peak at $B = 0$, is usually interpreted as weak antilocalization (WAL) due to spin-orbit interaction (SOI) [8].

In this Letter we show that the average magnetoconductance of mesoscopic systems built from two-dimensional hole gases (2DHG) distinctly deviates from the WL transmission dip profiles of their n-doped counterparts. Ballistic hole conductors such as circular quantum dots and Aharonov-Bohm (AB) rings, can exhibit a conductance peak at $B = 0$, even in the absence of SOI [9] due to structure (SIA) or bulk (BIA) inversion asymmetry.

Recently, various magnetotransport measurements on such high-mobility 2DHG have been performed for GaAs bulk samples [10], quasiballistic cavities [11], and AB rings [12,13]. However, we are not aware of corresponding theoretical approaches for ballistic 2DHG nanoconductors (except for 1D models [14]), despite the huge number of theory works on ballistic electron transport [15]. Here we treat 2DHG-based ballistic and diffusive mesoscopic structures on the level of the four-band Kohn-Luttinger Hamiltonian [16] for the two uppermost valence bands of a semiconductor: the heavy-hole (HH) and light-hole (LH) bands. By devising a semiclassical approach for ballistic dynamics in the coupled HH and LH bands, we can associate the anomalous WL features directly with Berry phases [17] in the Kohn-Luttinger model [18–20] (that have proven highly relevant, e.g., for the anomalous Hall [20] and spin Hall [21] effects). Such effects from HH-LH coupling (which is unrelated to SOI due to SIA and BIA) are hence of conceptional importance for a complete understanding of WL in 2DHG. They are *not* captured by effective two-band models usually used for the analysis of WL experiments [22]. We show that the strength of the related effective "Berry field," giving rise to effective TRS breaking at $B = 0$ and a splitting of the WL dip, is determined by a classical correlation between enclosed areas and reflection angles of interfering hole trajectories relevant for WL. This geometrical correlation is not amenable to existing random matrix approaches for chaotic conductors [15]. We confirm our semiclassical results by numerical transport calculations and discuss effects of SOI.

Hamiltonian and band structure.—To describe the 2DHG we represent the Kohn-Luttinger Hamiltonian [16] in an eigenmode expansion for a square well of width a modeling the vertical confinement [9]. Employing Löwdin partitioning [23] we construct an effective Hamiltonian based on the relevant, lowest subband in the z direction [22]. The resulting 4×4 Hamiltonian for a quasi-2DHG then describes coupled HH and LH states with spin projection $\pm 3/2$ and $\pm 1/2$, respectively. Without SOI due to SIA or BIA, the 2DHG Hamiltonian reads

$$\hat{\mathcal{H}}_{2\mathrm{D}} = \begin{pmatrix} \hat{P} & \hat{T} & & \\ \hat{T}^\dagger & \hat{Q} & & \\ & & \hat{Q} & \hat{T} \\ & & \hat{T}^\dagger & \hat{P} \end{pmatrix} = \begin{pmatrix} \hat{\mathcal{H}}_U & \\ & \hat{\mathcal{H}}_L \end{pmatrix}, \quad \begin{matrix} \mathrm{HH}\Uparrow \\ \mathrm{LH}\downarrow \\ \mathrm{LH}\uparrow \\ \mathrm{HH}\Downarrow \end{matrix} \tag{1}$$

with the upper and lower blocks composed of [24]

$$\hat{P} = -\frac{\hbar^2}{2m_0}[(\gamma_1 + \gamma_2)\hat{k}_\parallel^2 + (\gamma_1 - 2\gamma_2)\langle\hat{k}_z^2\rangle], \quad (2a)$$

$$\hat{T} = -\sqrt{3}\frac{\hbar^2}{2m_0}[\gamma_2(\hat{k}_x^2 - \hat{k}_y^2) + 2i\gamma_3\hat{k}_x\hat{k}_y], \quad (2b)$$

with $\hat{Q}(\gamma_1, \gamma_2) = \hat{P}(\gamma_1, -\gamma_2)$. Here, $\hat{\mathbf{k}} = (\hat{k}_x, \hat{k}_y, \hat{k}_z)$ is the wave vector with projection $\hat{k}_\parallel$ onto the xy plane of the 2DHG and $\langle\hat{k}_z^2\rangle = (\pi/a)^2$ is the expectation value of k_z for the lowest subband. Below we use the axial approximation, $\bar{\gamma} = \gamma_2 = \gamma_3$, for the parameters in $\hat{T}$ that couple HH and LH states. The band structure for the bulk and 2D case is shown and compared with an 8×8 Kane model [9] in [22]. Because of the 2D confinement the HH-LH bulk degeneracy is lifted [22] indicating enhanced HH-LH coupling which will play an important role for the WL analysis below. To this end we will calculate the two-terminal Landauer conductance

$$G = \frac{e^2}{h}T = \frac{e^2}{h}(T_U + T_L) = \frac{e^2}{h}\sum_{n,m}^{N}\sum_{\sigma,\sigma'}|t_{m,\sigma';n,\sigma}|^2 \quad (3)$$

with the transmission amplitudes $t_{m,\sigma';n,\sigma}$ given by the Fisher-Lee relations [25]. The indices m and n label N transverse modes in the leads, and $\sigma \in \{U, L\}$ with $U \in \{\text{HH}\Uparrow, \text{LH}\downarrow\}$ and $L \in \{\text{HH}\Downarrow, \text{LH}\uparrow\}$ denotes the HH and LH modes. The Hamiltonian (1) with blocks obeying $\hat{\mathcal{H}}_U(B) = \hat{\mathcal{H}}_L^\dagger(-B)$ allows us to separately define related total transmissions, T_U, T_L, fulfilling $T_U(B) = T_L(-B)$.

Depending on the Fermi level E_F we distinguish the case where HH and LH states are both occupied from the case where E_F is close to the band gap such that only HH states contribute to transport. We first study the latter case and focus on effects from the HH-LH coupling.

HH-LH coupling and Berry phase.—For ballistic mesoscopic systems of linear size L in the regime $kL \gg 1$, we will generalize the semiclassical approaches [26,27] to the Landauer conductance from electron systems with a parabolic dispersion to the p-doped case with more complex band topology. In particular, transport in the HH band will be affected by residual coupling to the LH band. The main effect of this coupling is to change the charge carriers' energy and phase. The change in their energies are well described by conventional perturbative approaches leading to new terms in the effective Hamiltonian, while the changes in their phases are conveniently accounted for in terms of a Berry curvature and associated Berry phases entering into the semiclassical dynamics [20,28]. In a momentum space representation, the geometrical phase Γ_σ, accumulated along a path during an adiabatic transition in k space associated with a reflection from a (smoothly varying) boundary potential, is given by [18,19]

$$\Gamma_\sigma = \int \mathcal{A}_\sigma(\boldsymbol{k})d\boldsymbol{k}; \quad \mathcal{A}_\sigma(\boldsymbol{k}) = -i\langle\psi_\sigma(\boldsymbol{k})|\nabla_k\psi_\sigma(\boldsymbol{k})\rangle. \quad (4)$$

This phase adds to the usual dynamical phase in the semiclassical treatment [see Eq. (8) below]. Using for $\psi_\sigma(\boldsymbol{k})$ the free solutions of Hamiltonian (1) we find after diagonalization for the vector potential

$$\mathcal{A}_{\text{HH}\Uparrow}(\boldsymbol{k}) = -\mathcal{A}_{\text{HH}\Downarrow}(\boldsymbol{k}) = 3\frac{\xi^{\text{Berry}}(k)}{k^2}\begin{pmatrix} k_y \\ -k_x \end{pmatrix}, \quad (5)$$

and $\mathcal{A}_{\text{LH}\downarrow}(\boldsymbol{k}) = -\mathcal{A}_{\text{LH}\uparrow}(\boldsymbol{k}) = -[(3\xi + 2)/3\xi]\mathcal{A}_{\text{HH}\Uparrow}(\boldsymbol{k})$ with $\xi^{\text{Berry}}(k) \simeq -\frac{1}{8}(\frac{ka}{\pi})^4$, to leading order in ka/π. The Berry phase for a reflection at a smooth boundary is then

$$\Gamma^{\text{Berry}}_{\text{HH}\Uparrow}(\varphi) = -\Gamma^{\text{Berry}}_{\text{HH}\Downarrow}(\varphi) = \xi^{\text{Berry}}\sin\varphi(2 - \cos\varphi), \quad (6)$$

where φ denotes the change in momentum direction.

For a specular reflection at a hard-wall (HW) confinement, a corresponding phase shift is obtained [22]:

$$\Gamma^{\text{HW}}_{\text{HH}\Uparrow}(\varphi) \overset{\xi^{\text{HW}} \ll 1}{\simeq} \xi^{\text{HW}}\sin 2\varphi; \quad \xi^{\text{HW}} \simeq -\frac{\gamma_1 + \bar{\gamma}}{4\bar{\gamma}}\left(\frac{ka}{\pi}\right)^2. \quad (7)$$

Average magnetoconductance.—A semiclassical approach proves convenient to incorporate these additional (Berry) phases into a theory of WL. For a (chaotic) ballistic dot the known semiclassical amplitude [26] for electron transmission from channel n to m is generalized to $t_{m,\text{HH}\Uparrow;n,\text{HH}\Uparrow} \simeq \sum_\gamma C_\gamma K_\gamma \exp(\frac{i}{\hbar}\mathcal{S}_\gamma)$, in terms of a sum over lead-connecting classical paths γ with classical action $\mathcal{S}_\gamma$, weight C_γ (including the Maslov index), and a factor $K_\gamma = \exp[i\sum_{j=1}^{n_b}\Gamma_{\text{HH}\Uparrow}(\varphi_j)]$ accounting for the accumulated phases (6) or (7) after n_b successive reflections. In view of Eq. (3) the total semiclassical transmission probability for HH $\Uparrow$ states reads

$$T_U \simeq \sum_{n,m}\sum_{\gamma\gamma'} K_\gamma K_{\gamma'}^* C_\gamma C_{\gamma'}^* e^{(i/\hbar)(\mathcal{S}_\gamma - \mathcal{S}_{\gamma'})}. \quad (8)$$

The diagonal term, $\gamma = \gamma'$, yields the classical transmission [26] since the phases cancel and $K_\gamma K_\gamma^* = 1$.

In the following we consider WL contributions which arise as quantum interference effects (after averaging) from off-diagonal pairs of long, classically correlated paths $\gamma \neq \gamma'$ with small action difference ($\mathcal{S}_\gamma - \mathcal{S}_{\gamma'} \sim \hbar$), where γ forms a loop and γ' follows the loop in the opposite direction while it coincides with γ for the rest of the trajectory [27]. Because of the time-reversed traversal of the loop the two paths acquire, in the presence of a magnetic field B, an additional action difference $(\mathcal{S}_\gamma - \mathcal{S}_{\gamma'})/\hbar = 4\pi AB/\Phi_0$, where A is the enclosed (loop) area and Φ_0 the flux quantum. Moreover, during the loop γ and γ' have opposite reflections, $\varphi_j = -\varphi_j'$, and hence $K_\gamma K_{\gamma'}^* = \exp[2i\sum_{j=1}^{n_b}\Gamma_{\text{HH}\Uparrow}(\varphi_j)]$. For chaotic dynamics in a cavity where the escape length L_{esc} is much larger than the average distance L_b between consecutive bounces, we can introduce probability distributions for the areas A and the phases $\sum_{j=1}^{n_b}\Gamma_{\text{HH}\Uparrow}(\varphi_j)$. Our classical simulations for both the smooth and the HW case revealed that the probability distributions of $\sum_{j=1}^{n_b}\Gamma_{\text{HH}\Uparrow}(\varphi_j)$ coincide very well (for $n_b > 5$ and $\xi < 1$) with the distribution $\tilde{\xi}\sum_{j=1}^{n_b}\varphi_j$ with a renormalized HH-LH coupling $\tilde{\xi}^{\text{Berry}} \simeq 0.6\xi^{\text{Berry}}$ and

$\tilde{\xi}^{\mathrm{HW}} \simeq 0.2\xi^{\mathrm{HW}}$. This allows us to treat both cases on equal footing using $K_\gamma K^*_{\gamma'} = e^{2i\tilde{\xi}\alpha}$ with $\alpha = \sum_{j=1}^{n_b} \varphi_j$.

Generalizing the semiclassical approaches for electron [26,27] to HH ⇑ (⇓) transport, the WL correction can then be expressed as an integral over trajectory lengths,

$$\delta T_{U(L)} = \frac{\delta T^{(0)}}{L_{\mathrm{esc}}} \int_0^\infty e^{-L/L_{\mathrm{esc}}} \mathcal{M}(L; B, \mp\tilde{\xi}) dL. \quad (9)$$

Here $\delta T^{(0)}$ denotes WL for $B = 0$, $\tilde{\xi} = 0$ [$\delta T^{(0)} = -1/(4 - 2/N)$ for chaotic electronic conductors [15]], and

$$\mathcal{M}(L; B, \tilde{\xi}) = \int_{-\infty}^{\infty} dA \int_{-\infty}^{\infty} d\alpha P_L(A, \alpha) e^{2\pi i[\tilde{\xi}\alpha/\pi + 2AB/\Phi_0]}, \quad (10)$$

where $P_L(A, \alpha)$ is the joint probability distribution for the accumulated areas and angles. While both parameters follow Gaussian distributions, we stress that there exist nonuniversal correlations between A and α reflecting the geometry of the quantum dot. When plotting $P_L(A, \alpha)$ these correlations show up as deviations from a circular symmetry, as illustrated in Fig. 1(a), showing classical simulations for a chaotic cavity [inset of Fig. 3(a)].

The central limit theorem implies a two-dimensional multivariate normal distribution,

$$P_L(A, \alpha) \propto \exp\left[-\frac{(A/A_0)^2 + (\alpha/\alpha_0)^2 - 2\rho A\alpha/(A_0\alpha_0)}{2(1-\rho^2)L/L_b} \right]. \quad (11)$$

Correlations are encoded in ρ ranging from 0 to ± 1. Assuming ergodicity we obtain for the variances of the angle $\alpha_0^2 = 4(\pi - 2)$, area $A_0^2 \simeq \frac{2}{15}[L_b^2 + \mathrm{var}(L_b)]^2$, and covariance $\rho A_0\alpha_0 = L_b^2(\frac{\pi}{4} - \frac{1}{3})$. This leads to the geometry-dependent $\rho \simeq 0.58/[1 + \mathrm{var}(L_b)/L_b^2]$, i.e., $\rho < 0.58$ for a chaotic system. [$\rho \approx 0.5$ for the cavity in Fig. 3(a).] The correlations can be stronger in nonchaotic systems and are pronounced for a disk [inset of Fig. 3(b)] as we see in Fig. 1(b). (We find $\rho \approx 0.8$.)

Using Eqs. (10) and (11), we get from Eq. (9) semiclassically a Lorentzian WL dip magnetoconductance profile

$$\delta T_{U(L)}(B) = \frac{\beta\delta T^{(0)}}{1 + [2\pi\sqrt{2\beta}A_0(B \mp B_{\mathrm{Berry}})/\Phi_0)]^2 L_{\mathrm{esc}}/L_b}, \quad (12)$$

with a depth $\delta T_{U(L)}(B_{\mathrm{min}}) = \beta\delta T^{(0)}$, with

$$\beta = [1 + 2\alpha_0^2(1-\rho^2)\tilde{\xi}^2 L_{\mathrm{esc}}/L_b]^{-1}. \quad (13)$$

As a main result, the WL dip is shifted by the Berry field

$$B_{\mathrm{Berry}} = \rho\tilde{\xi}\alpha_0\Phi_0/(2\pi A_0), \quad (14)$$

which relies on both *quantum* HH-LH coupling $\tilde{\xi}$ and finite *classical* A-α correlations ρ.

In Figs. 2(a) and 2(b) we compare our predictions (13) and (14) for the dip depth, $\delta T_U(B_{\mathrm{min}}) = -\beta/(4 - 2/N)$, and displacement, B_{Berry}, with numerical recursive Green function calculations [29] of these quantities for a chaotic quantum dot [inset of Fig. 3(a)] for different HH-LH couplings by tuning the vertical confinement a. The numerics (symbols) show quantitative agreement with the semiclassical curves (lines), which are entirely based on the classical parameters A_0, α_0, and ρ.

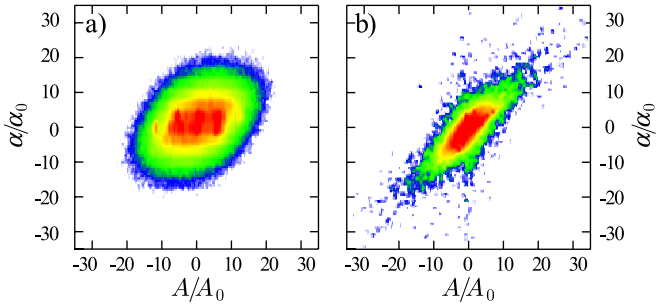

FIG. 1 (color online). Probability distributions to find an orbit with enclosed area A and accumulated angle α for (a) a chaotic cavity [inset of Fig. 3(a)] and (b) a disk [inset of Fig. 3(b)]. [Central (red) regions correspond to high probability.]

Finally, we analyze in the central Fig. 3 the effect of the geometrical correlation ρ on WL in different representative mesoscopic systems for fixed, realistic HH-LH coupling. Figure 3(a) depicts the WL profile of a chaotic cavity. Our semiclassical results (without free parameters) show remarkable agreement with the quantum calculations. The nonzero $\rho \approx 0.5$ gives rise to a splitting of the T_U and T_L traces by $2B_{\mathrm{Berry}}$ leading to a flattened WL dip for $T_U + T_L$ compared to the Lorentzian WL profile for electrons. Figure 3(b) shows results for the circular dot with larger correlation ($\rho \approx 0.8$). Accordingly, the Berry field is stronger leading to a WAL-type overall profile. Correspondingly, we find in the averaged transmission of AB rings [Fig. 3(c)] distinct additional features at $B = 0$ absent in electron transport (see also [14]).

We close with several remarks.

(i) Corresponding transport calculations for dots with smooth confinement yield a ka scaling of B_{Berry} close to the quartic behavior predicted by ξ^{Berry} from Eq. (5).

(ii) The correlation mechanism is not restricted to ballistic systems but is also relevant in diffusive ones, as illustrated in Fig. 3(d), leading to broadening and deviations of the WL profile from that of a digamma function for electrons.

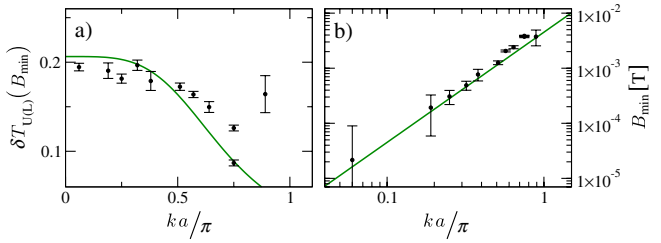

FIG. 2 (color online). Dependence of (a) the depth $\delta T_{U(L)}(B_{\mathrm{min}})$ and (b) the position B_{min} of the magnetotransmission weak localization dip on ka [governing the effective HH-LH coupling, see Eq. (7)] for HH transport through a chaotic quantum dot [inset of Fig. 3(a)]. Numerical quantum results (symbols) are compared to the semiclassical predictions (13) and (14), [(green) lines] for $\gamma_1 = 6.85$, $\bar{\gamma} = 2.5$ (for GaAs).

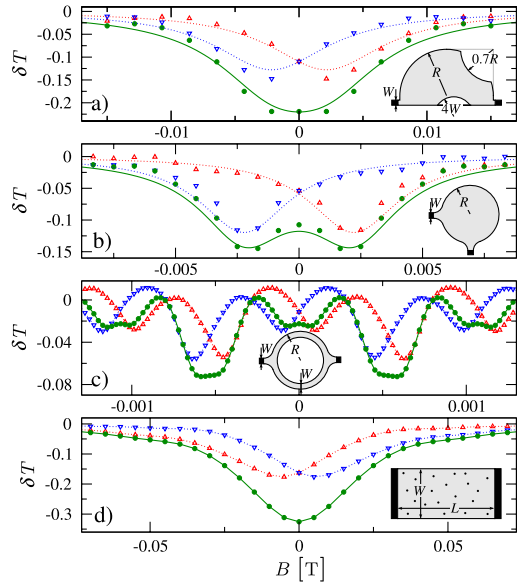

FIG. 3 (color online). HH-LH coupling-induced Berry phase effects on weak localization in various mesoscopic hole gases. The WL correction δT is shown for a ballistic chaotic cavity (a), disk (b), AB ring (c), and a diffusive strip (d). Red ($\triangle$) and blue ($\triangledown$) triangles denote quantum mechanical transmissions $\delta T_U(B)$, $\delta T_L(B)$ adding up to the full $\delta T(B)$ [green bullets, see text below Eq. (3)]. The red and blue dotted curves in (a) and (b) show our semiclassical results (12) with the horizontal displacements given by the Berry field (14) reflecting geometrical correlations [based on the calculated classical quantities $A_0 \simeq 12\,200$ [56 129] nm^2, $\alpha_0 \simeq 1.92$ [5.89], $\rho \simeq 0.5$ [0.8] in (a) [(b)]]. In (c), (d) the lines are guides to the eye of the quantum results. See [22] for the parameters used.

(iii) If HH and LH states are both occupied and contribute to transport, our quantum calculations show a *vanishing* WL correction both for diffusive and chaotic ballistic conductors due to effective TRS breaking in the individual subblocks, which, as far as we know, has not been reported before. It is notable that this kind of effective TRS breaking, recently discussed in the context of graphene and topological insulators [30], is already present in the well-established system of a 2DHG. Interestingly, if only HH states are occupied, TRS breaking in each subblock can be traced back to the Berry field (14); i.e., system-specific classical correlations determine the degree of TRS breaking, and hence the mere knowledge of the overall universality class is insufficient.

(iv) SOI terms due to SIA and BIA couple the subblocks, eventually restore TRS, and give rise to WAL effects on top of the mechanisms illustrated in Fig. 3; we checked this numerically for BIA for the diffusive and ballistic case. Hence in 2DHG-based AB measurements such as [12,13] presumably both SOI and HH-LH coupling-induced phases affect the AB signal. The latter mechanism should be more clearly observable in systems with reduced SOI such as WL studies in Si [31]. Moreover these WAL effects might also be visible in p-doped ferromagnetic semiconductors such as GaMnAs [32].

(v) We found equivalent Berry phase-induced WL phenomena also in quantum transport through HgTe-based quantum wells with SOI [22].

We acknowledge funding through the Deutsche Forschungsgemeinschaft [DFG-JST Forschergruppe on Topological Electronics (K. R.) and project KR-2889/2 (V. K.)], DAAD (M. W.), TUBA under Grant No. I.A/TUBA-GEBIP/2010-1 (I. A.), and the A. von Humboldt Foundation (J. K.).

[1] B. W. Hapke, R. M. Nelson, and W. D. Smythe, Science **260**, 509 (1993).
[2] M. P. Van Albada and A. Lagendijk, Phys. Rev. Lett. **55**, 2692 (1985); P.-E. Wolf and G. Maret, *ibid.* **55**, 2696 (1985).
[3] E. Larose *et al.*, Phys. Rev. Lett. **93**, 048501 (2004).
[4] G. Bayer and T. Niederdränk, Phys. Rev. Lett. **70**, 3884 (1993).
[5] M. Hartung *et al.*, Phys. Rev. Lett. **101**, 020603 (2008).
[6] E. Abrahams *et al.*, Phys. Rev. Lett. **42**, 673 (1979).
[7] B. L. Altshuler *et al.*, Phys. Rev. B **22**, 5142 (1980).
[8] A. L. S. Hikami and Y. Nagaoka, Prog. Theor. Phys. **63**, 707 (1980).
[9] R. Winkler, *Spin-Orbit Coupling Effects in Two-Dimensional Electron and Hole Systems* (Springer, Berlin, 2003).
[10] S. McPhail *et al.*, Phys. Rev. B **70**, 245311 (2004).
[11] S. Faniel *et al.*, Phys. Rev. B **75**, 193310 (2007).
[12] J.-B. Yau, E. P. De Poortere, and M. Shayegan, Phys. Rev. Lett. **88**, 146801 (2002).
[13] B. Grbić *et al.*, Phys. Rev. Lett. **99**, 176803 (2007).
[14] M. Jääskeläinen and U. Zülicke, Phys. Rev. B **81**, 155326 (2010).
[15] C. W. J. Beenakker, Rev. Mod. Phys. **69**, 731 (1997).
[16] J. M. Luttinger and W. Kohn, Phys. Rev. **97**, 869 (1955).
[17] M. V. Berry, Proc. R. Soc. A **392**, 45 (1984).
[18] M.-C. Chang and Q. Niu, Phys. Rev. B **53**, 7010 (1996).
[19] F. D. M. Haldane, Phys. Rev. Lett. **93**, 206602 (2004).
[20] M.-C. Chang and Q. Niu, J. Phys. Condens. Matter **20**, 193202 (2008).
[21] S. Murakami, N. Nagaosa, and S.-C. Zhang, Science **301**, 1348 (2003).
[22] See supplemental material at http://link.aps.org/supplemental/10.1103/PhysRevLett.106.146801 for models of the hole gas band structure, related Berry phases, and weak localization in HgTe cavities.
[23] P.-O. Löwdin, J. Chem. Phys. **19**, 1396 (1951).
[24] D. A. Broido and L. J. Sham, Phys. Rev. B **31**, 888 (1985).
[25] D. S. Fisher and P. A. Lee, Phys. Rev. B **23**, 6851 (1981).
[26] H. U. Baranger, R. A. Jalabert, and A. D. Stone, Phys. Rev. Lett. **70**, 3876 (1993); Chaos **3**, 665 (1993).
[27] K. Richter and M. Sieber, Phys. Rev. Lett. **89**, 206801 (2002).
[28] M. P. Marder, *Condensed Matter Physics* (Wiley, New York, 2000).
[29] M. Wimmer and K. Richter, J. Comput. Phys. **228**, 8548 (2009).
[30] B. A. Bernevig, T. L. Hughes, and S. H. Zhang, Science **314**, 1757 (2006).
[31] A. Yu. Kuntsevich *et al.*, Phys. Rev. B **75**, 195330 (2007).
[32] D. Neumaier *et al.*, Phys. Rev. Lett. **99**, 116803 (2007).